

AGN HOST GALAXIES AT $Z \sim 0.4$ – 1.3 : BULGE-DOMINATED AND LACKING MERGER–AGN CONNECTION

N. A. GROGIN¹, C. J. CONSELICE², E. CHATZICHRISTOU³, D. M. ALEXANDER⁴, F. E. BAUER⁵, A. E. HORNSCHEMEIER¹, S. JOGEE⁶, A. M. KOEKEMOER⁷, V. G. LAIDLER⁷, M. LIVIO⁷, R. A. LUCAS⁷, M. PAOLILLO⁸, S. RAVINDRANATH⁷, E. J. SCHREIER⁹, B. D. SIMMONS³, AND C. M. URRY³

Astrophysical Journal Letters, in press

ABSTRACT

We investigate morphological structure parameters and local environments of distant moderate-luminosity active galactic nucleus (AGN) host galaxies in the overlap between the *HST*/ACS observations of the Great Observatories Origins Deep Survey (GOODS) and the two Chandra Deep Fields. We compute near-neighbor counts and *BViz* asymmetry (A) and concentration (C) indices for $\approx 35,500$ GOODS/ACS galaxies complete to $z_{850} \approx 26.6$, including the resolved hosts of 322 X-ray-selected AGNs. Distributions of (1) z_{850} asymmetry for 130 $z_{850} < 23$ AGN hosts and (2) near-neighbor counts for 173 $z_{850} < 24$ AGN hosts are both consistent with non-AGN control samples. This implies no close connection between recent galaxy mergers and moderate-luminosity AGN activity out to appreciable look-back times ($z \lesssim 1.3$), approaching the epoch of peak AGN activity in the universe. The distribution of z_{850} C for the AGN hosts is offset by $\Delta C \approx +0.5$ compared to the non-AGN, a 6.4σ discrepancy much larger than can be explained by the possible influence of unresolved emission from the AGN or a circumnuclear starburst. The local universe association between AGN and bulge-dominated galaxies thus persists to substantial look-back time. We discuss implications in the context of the low-redshift supermassive central black hole mass correlation with host galaxy properties, including concentration.

Subject headings: galaxies: active—galaxies: structure—surveys—X-rays: galaxies

1. INTRODUCTION

The connection between active galactic nuclei (AGNs) and their host galaxies, and the evolution in that relationship over cosmic time, have attracted great interest in recent years. This includes the discoveries that most nearby massive galaxies harbor central supermassive black holes (SMBHs; Magorrian et al. 1998), that AGNs in the local universe ($z \lesssim 1$) reside predominantly in massive, bulge-dominated host galaxies (Kauffmann et al. 2003), and that a tight correlation exists locally between SMBH mass and host galaxy properties such as bulge velocity dispersion and light-profile concentration (Ferrarese & Merritt 2000; Gebhardt et al. 2000; Graham et al. 2001). The 1–2 Ms Chandra Deep Fields (CDF-N and CDF-S; Brandt et al. 2001; Giacconi et al. 2002), which have now resolved much of the cosmic X-ray background into moderate-luminosity AGNs at $z \sim 1$ (Alexander et al. 2003; Barger et al. 2003; Szokoly et al. 2004), provide a unique AGN sample to probe these

locally observed SMBH-host relationships out to epochs nearing the peaks of star formation and AGN activity in the universe. This is one of the aims of the Great Observatories Origins Deep Survey (GOODS; Giavalisco et al. 2004), which has obtained deep multicolor *Hubble Space Telescope* (*HST*) Advanced Camera for Surveys (ACS) image mosaics across the most sensitive regions of the CDF areas. In this Letter we report on the local environments and rest-frame optical morphologies of AGN host galaxies in the GOODS fields as well as the implications for SMBH-galaxy coevolution and the merger-AGN connection.

The largest pre-GOODS investigation of *HST*-imaged CDF sources was Koekemoer et al. (2002), with 41 CDF-S 1 Ms sources in three moderately deep Wide Field Planetary Camera 2 (WFPC2) pointings. Grogin et al. (2003, hereafter G03) studied the *HST* morphologies and local environments of these faintest X-ray sources as compared with the X-ray undetected population. The AGNs were preferentially located in galaxies with highly concentrated light profiles, but the AGN hosts could not be differentiated from the non-AGN based on light-profile asymmetry or frequency of near-neighbors. The G03 conclusions were as follows: (1) distant moderate-luminosity AGNs did not show a connection between recent ($\lesssim 1$ Gyr) galaxy merger/interaction and AGN activity; and (2) the $z \sim 1$ galaxy population already showed evidence of the SMBH-bulge correlation. Now that deeper and much larger area GOODS imaging is available across both CDFs, we verify these results with much larger samples of both CDF AGNs and quiescent galaxies. We also place new constraints on the *evolution* in merger-AGN connection and SMBH-bulge correlation with the extensive redshift information now accumulated

¹ Department of Physics and Astronomy, Johns Hopkins University, Charles and 34th Street, Baltimore, MD 21218.

² Department of Astronomy, California Institute of Technology, 1201 East California Boulevard, Pasadena, CA 91125.

³ Department of Astronomy, Yale University, P.O. Box 208101, New Haven, CT 06520-8101.

⁴ Institute of Astronomy, Madingley Road, Cambridge CB3 0HA, UK.

⁵ Department of Astronomy, Columbia University, 550 W. 120th Street, New York, NY 10027.

⁶ Department of Astronomy, University of Texas, 1 University Station, C1400, Austin, TX 78712-0259.

⁷ Space Telescope Science Institute, 3700 San Martin Drive, Baltimore, MD 21218.

⁸ Dipartimento di Scienze Fisiche, Università degli Studi Federico II, C. U. Monte S. Angelo, via Cintia, I-80126 Naples, Italy.

⁹ Associated Universities, Inc., 1400 16th Street, NW, Washington, DC 20036.

in these fields. We adopt a cosmology with $H_0 = 70 \text{ km s}^{-1} \text{ Mpc}^{-1}$, $\Omega_m = 0.3$, and $\Omega_\Lambda \equiv 1 - \Omega_m = 0.7$. Magnitudes are given in the AB system.

2. OBSERVATIONS AND SAMPLE SELECTION

Our analyses employ the *HST*/ACS image mosaics in F606W (V), F775W (i), and F850LP (z_{850}) from the first three epochs of GOODS *HST* observations in both the northern (“GOODS-N”) and southern (“GOODS-S”) fields (Giavalisco et al. 2004). We use the z_{850} -detected source catalog detailed in Ravindranath et al. (2004), trimmed by applying minimum thresholds in compactness (> 4 pixels) and signal-to-noise ratio (> 5) optimized for removing spurious detections. The remaining 16,632 GOODS-S sources and 18,878 GOODS-N sources are complete to $z_{850} \approx 26.6$ and form the basis of our environmental and structural parameter analyses.

We identify candidate AGN hosts from source catalogs of the 1 Ms CDF-S and 2 Ms CDF-N X-ray images reduced and source-extracted in a consistent fashion (Alexander et al. 2003). These two X-ray surveys provide the deepest views of the universe in the 0.5–8.0 keV band. Within the respective GOODS-N(S) areas, the CDF-N(S) contains 324(223) X-ray sources down to comparable sensitivity limits of $\approx 1.0(1.3) \times 10^{-16} \text{ ergs s}^{-1} \text{ cm}^{-2}$ at 0.5–2.0 keV and $\approx 7.2(8.9) \times 10^{-16} \text{ ergs s}^{-1} \text{ cm}^{-2}$ at 2–8 keV. Coordinate-matching to the z_{850} catalog yields unambiguous counterparts for $> 80\%$ of the CDF sources (F. E. Bauer et al. 2005, in preparation). Many are comparatively nearby and optically bright starbursts and “quiescent” galaxies contaminating our desired X-ray-selected AGN sample. The extensive redshift coverage of $z_{850} \lesssim 24$ CDF counterparts allows us to exclude these non-AGNs with a luminosity threshold of $L(2\text{--}8 \text{ keV}) > 10^{42} \text{ ergs s}^{-1}$. The resulting L_X -limited AGN sample of 322 galaxies contains few CDF sources at $z < 0.4$, so we choose this as our lower limit for redshift-evolution analyses (§5).

We investigate evolutionary trends in morphology and environment among the GOODS AGN and non-AGN populations by constructing complete volume-limited subsamples. We estimate absolute magnitudes for the GOODS-S galaxies by using the photometric redshift database of Mobasher et al. (2004), who claim an accuracy of $\Delta z/(1+z) \lesssim 0.1$ at $z_{850} \lesssim 24.5$ for AGN and non-AGN alike. Although we lack a comparable photometric redshift database for the GOODS-N field, redshift measurements of the CDF-N sources (Fernandez-Soto, Lanzetta, & Yahil 1999; Cohen et al. 2000; Barger et al. 2003) are largely complete to a similar depth ($z_{850} \lesssim 24.5$). Hence, we include another 135 CDF-N sources with measured redshifts for our volume-limited AGN sample.

To probe the evolution of the *optical* morphology of AGN hosts versus the field, we compute rest-frame B -band (hereafter B_0) quantities out to the limit $z < 1.3$ accessible to our reddest filter (z_{850}). To estimate M_B and the B_0 structural parameters, we linearly interpolate between V and i for galaxies at $0.31 < z \leq 0.73$, between i and z_{850} for $0.73 < z \leq 1.09$, and use z_{850} quantities for $1.09 < z < 1.3$. The redshift survey limit of $z_{850} \approx 24.5$ corresponds to $M_B \approx -19.5$ at $z = 1.3$. We adopt this as our limiting absolute magnitude, satisfied by 1090 GOODS-S galaxies in the non-AGN sample

and another 37(42) AGN hosts from CDF-N(S). These volume-limited samples probe to ≈ 1 mag fainter than L_* and thus are not restricted to the highest luminosity galaxies. Coincidentally, $z \sim 1.3$ is the limit for *Chandra* detection of $L(2\text{--}8 \text{ keV}) > 10^{42} \text{ ergs s}^{-1}$ sources throughout the GOODS regions. As a result, our AGN sample is essentially complete.

3. CONCENTRATION AND ASYMMETRY INDICES

We quantify the GOODS galaxy morphologies via non-parametric indices of concentration C and asymmetry A (Conselice 2003 and references therein). Index C scales with the ratio of radii containing 80% and 20% of a source’s total flux, $C \equiv 5 \log(r_{0.8}/r_{0.2})$, and increases toward bulge-dominated morphologies. Index A is the flux-normalized residual of the source pixels S differenced with their 180° -rotated counterpart S_{180} : $A \equiv \min \left(\sum_{\text{pix}} |S - S_{180}| / \sum_{\text{pix}} |S| \right) - A_0$, where A_0 is a background term and the minimization is over a 0.2 pixel grid of possible centers of rotation. While A moderately increases toward disk-dominated morphologies, it is driven to large values ($A \gtrsim 0.35$) for galaxies with recent or ongoing interaction.

Figure 1 shows the z_{850} indices C (*top panel*) and A (*bottom panel*) for resolved sources in both GOODS fields versus z_{850} magnitude.

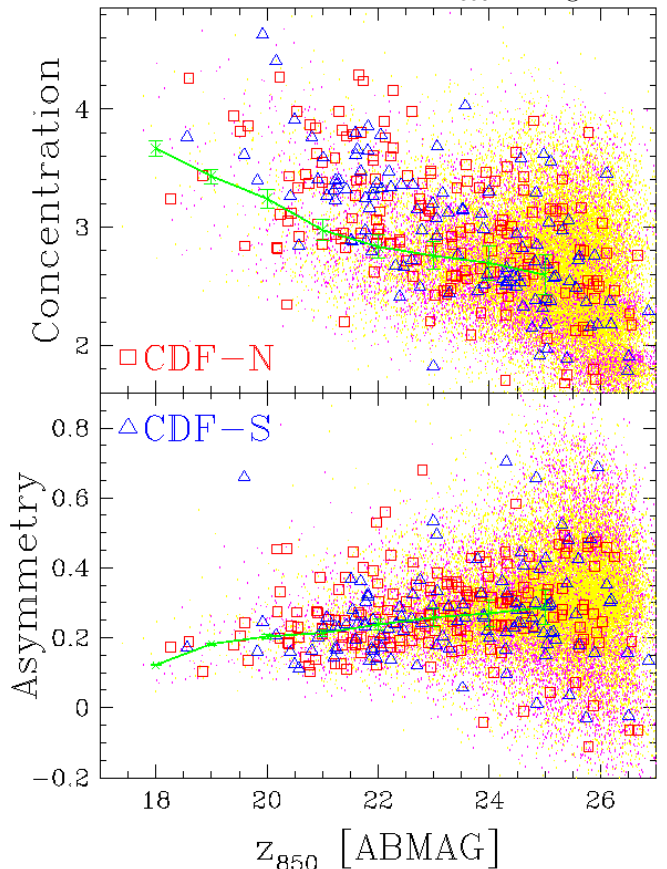


FIG. 1.— Concentration index (*top*) and asymmetry index (*bottom*) vs. magnitude as measured in z_{850} for resolved GOODS sources. The large symbols represent the AGN sample in the north (*red squares*) and south (*blue triangles*); the small dots represent the non-AGNs in the north (*yellow*) and south (*magenta*). The connected green crosses and their error bars denote the median values and measurement errors for the non-AGNs in successive 1 mag bins.

The asymmetries of the AGN hosts (*large symbols*) and non-AGN (*small dots*) are not clearly separated. However the AGN host concentrations clearly populate the upper end of the field distribution throughout the regime of good signal-to-noise ratio ($z_{850} \lesssim 24$). Such large C -values are preferentially associated with massive early-type galaxies, although we note that the AGN hosts span a broad range of morphology (e.g., Koekemoer et al. 2002). The declining C with host magnitude is interpreted as an evolutionary effect; galaxies at higher redshift (and thus generally fainter) are intrinsically less concentrated (Conselice et al. 2003). When comparing the C distributions for z_{850} -limited samples of AGN and non-AGN (§5.1), we compensate for this magnitude-dependent bias in C by resampling the non-AGN population to match the AGN hosts’ magnitude distribution.

4. NEAR-NEIGHBOR FREQUENCY

In assessing the role of environment in AGN activity, we complement the A analysis with a comparison of the near-neighbor counts around $z_{850} < 24$ AGN hosts versus the non-AGN. Qualifying neighbors must satisfy both proximity and relative brightness criteria. We investigate two different definitions of proximity threshold d : one that scales with the Petrosian radius r_P of the primary galaxy, $d < 3r_P$, and another that remains fixed for all galaxies, $d < 8''$. The latter choice, consistent with the analysis of G03, corresponds to 54 kpc at $z = 0.6$ and varies by only $\pm 25\%$ over the range $0.4 < z < 1.3$.

To limit contamination of the neighbor statistics by chance superpositions of background galaxies, a neighbor is rejected if more than 2 mag fainter than the comparison galaxy. This relative magnitude cutoff, in the presence of steeply increasing galaxy number counts with magnitude, introduces a bias towards more neighbors around fainter galaxies. When comparing AGN and non-AGN near-neighbor counts, we therefore resample the non-AGN to match the magnitude distribution of the AGN hosts, analogous to the procedure used in comparing C distributions (§3). Because the resolved CDF optical counterparts typically show only minor flux contribution from the active nucleus (G03), the relative faintness of qualifying AGN neighbors is not significantly biased with respect to the non-AGN. We discuss the similarity of the AGN and non-AGN near-neighbor frequency histograms in §5.2.

5. DISCUSSION

5.1. Bulge-dominated AGN Hosts at $z \sim 0.4\text{--}1.3$

The top left panel of Figure 2 notes the Kolmogorov-Smirnov (K-S) test probabilities for the null hypothesis that the $z_{850} < 23$ AGN host and non-AGN C -values could be drawn from the same underlying distribution. The quoted probabilities are the median values from 1000 resamplings of the non-AGN sample matched to the magnitude distribution of $z < 23$ AGN hosts to remove magnitude-dependent C bias (see §3). The C distributions are highly inconsistent at the 6.4σ level ($P_{K-S} = 1.6 \times 10^{-10}$). Moreover, both the northern and the southern $z_{850} < 23$ AGN host concentrations are individually discrepant with their respective non-AGN counterparts at $P_{K-S} < 10^{-6}$.

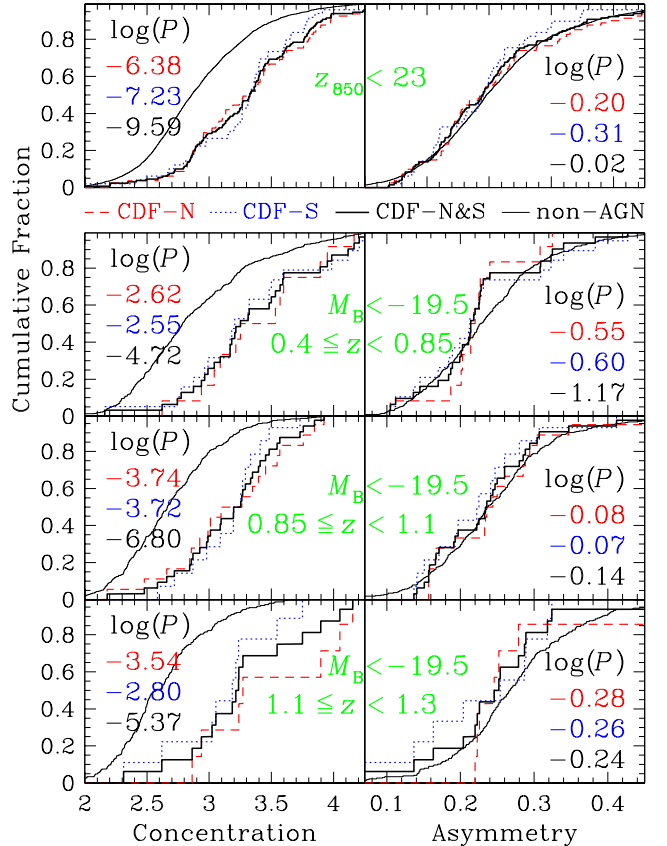


FIG. 2.— Cumulative distribution functions of concentration index (*left panels*) and asymmetry index (*right panels*) for resolved GOODS AGN hosts from the CDF-S (*dotted blue line*), CDF-N (*dashed red line*), and the combination of both CDFs (*thick solid black line*) for a flux-limited sample (*top row*) and a volume-limited sample divided into three redshift bins (*bottom three rows*). The indices are compared in z_{850} for the flux-limited sample, and in (interpolated) rest-frame B for the volume-limited sample. Null-hypothesis probabilities P from K-S comparisons with the control sample of non-AGN GOODS-South galaxies (*thin solid black line*) are also noted in each panel.

The median C offset of +0.5 is consistent with the G03 measurement based on $I < 23$ sources in three *HST*/WFPC2 pointings in the CDF-S (including 25 X-ray-detected sources) and far exceeds the ~ 0.1 enhancement in C expected from nuclear point-source optical flux in the AGN sample (see G03). Moreover, C enhancement by potential circumnuclear starbursts is discounted because (1) *unresolved* starbursts reduce to the previous case for AGN point-source contamination and (2) resolved ($\gtrsim 500$ pc) central starbursts with sufficient flux to bias C would be inconsistent with the low incidence of starburst-type spectral energy distributions (SEDs) among the GOODS AGN hosts as compared to the field (Mobasher et al. 2004).

The traditional conception of “local AGN \equiv Seyfert \equiv late-type host” has been refuted by the Kauffmann et al. (2003) analysis of thousands of spectroscopically identified low-redshift ($z \lesssim 0.3$) AGN host galaxies from the Sloan Digital Sky Survey (SDSS). Local AGN of all luminosities reside almost exclusively in massive hosts with sizes, stellar mass densities, and concentration indices similar to ordinary early-type SDSS galaxies. The enhanced C among the GOODS AGN hosts now indicates that nuclear activity remains preferentially asso-

ciated with bulge-dominated galaxies out to substantial lookback times ($z < 1.3$). Our $z \sim 0.4$ – 1.3 sample largely bridges the span of cosmic time between the quasar epoch, where accretion-driven luminosity is dominated by high-mass SMBHs, and the recent-epoch AGN hosts probed by SDSS. If the locally-observed tight correlation between SMBH mass and host C (Graham et al. 2001) similarly extends to $z \sim 0.4$ – 1.3 , then our results newly suggest that the accretion-driven luminosity of the universe is dominated by the most massive SMBHs at virtually all times.

The discovery of an epoch beyond which SMBH mass and host-galaxy properties (including C) lose their tight correlation could strongly constrain theories of SMBH and host-galaxy co-evolution. To ascertain if the C discrepancy between AGN and non-AGN shows any evolution with redshift, we divide our volume-limited sample into three redshift bins spanning ≈ 550 Mpc³ each: $0.4 \leq z < 0.85$, $0.85 \leq z < 1.1$, and $1.1 \leq z < 1.3$. The AGN host C is clearly elevated in all three bins (Fig. 2, *three bottom left panels*), reflected in the persistently low $\log P_{K-S} \sim -6.8$ to -4.7 . Thus our GOODS AGN host-galaxy sample populates the high end of both the L_X distribution (by construction) and the C distribution throughout the range $0.4 < z < 1.3$. Pushing this analysis beyond $z \approx 1.3$ faces multiple obstacles, including (1) identification of obscuration-unbiased moderate-luminosity AGNs ($L_X > 10^{42}$ ergs s⁻¹), requiring *Chandra* exposure depths of *several* megaseconds; (2) construction of a large, complete $M_B \leq -19.5$ field sample in the so-called redshift desert; and (3) well-resolved rest-frame optical light profiles out to meaningful isophotes, requiring $\sim 0''.1$ resolution *J*-band imaging at extreme depths to overcome the sharply increasing surface brightness dimming.

Although tantalizing to conclude that the Graham et al. (2001) SMBH-bulge correlation now persists to $z < 1.3$, it is unclear whether L_X is a reasonable proxy for SMBH mass at these redshifts. At low redshift, AGNs with well-constrained SMBH mass are observed to have (1) $L_X \lesssim L_{\text{Edd}} \propto M_{\text{BH}}$, but with a large scatter to lower Eddington ratios (Woo & Urry 2002) and (2) an AGN fundamental plane in L_X , L_{Radio} , and M_{BH} , but poor correlation between L_X and M_{BH} individually (Merloni et al. 2003). However Barger et al. (2005) have recently claimed a tight L_X - M_{BH} correlation at $z \sim 1$. Direct measurement of the SMBH masses of GOODS galaxies would be ideal but extremely challenging for moderate-luminosity (and often dust-obscured) AGNs at these redshifts.

5.2. No Merger-AGN Connection at $z \sim 0.4$ – 1.3 ?

Unlike the disparate C distributions, the asymmetry indices of the 130 resolved $z_{850} < 23$ GOODS AGN hosts are statistically indistinguishable from the non-AGN ($P_{K-S} = 0.97$). This result reinforces the G03 findings based on a subset of 25 X-ray-detected sources with $I < 23$. Figure 2 (*right panels*) shows that this similarity in A exists in B_0 throughout all three redshift bins and separately among northern and southern AGN subsamples. The lowest of the K-S test probabilities, for the combined AGN sample at $0.4 \leq z < 0.85$, does not exceed a 2σ rejection of the null hypothesis.

Recent/ongoing galaxy mergers in the local universe

generally have large A enhancement ($A > 0.35$; Conselice et al. 2003). Furthermore, N -body simulations suggest that even minor mergers have significant A enhancement up to 1 Gyr from the onset of the merger (Walker, Mihos & Hernquist 1996). The lack of differentiation between AGN and non-AGN A distributions therefore implies that recent merging/interaction is no more prevalent among the AGNs. This in turn argues against the hypothesis that AGN fueling is directly linked to recent ($\lesssim 1$ Gyr) galaxy merging/interaction, while favoring mechanisms such as low-level gas accretion from the intergalactic medium and/or bar instability in disks.

HST imaging of 20 nearby ($z < 0.3$) quasars by Bahcall et al. (1997) suggested that galaxy mergers/interactions are relatively common among the highest luminosity AGNs ($\gtrsim 10^{44.5}$ ergs s⁻¹). However, our finding of no A enhancement among more distant ($z \sim 0.4$ – 1.3) AGNs at lower luminosities ($\lesssim 10^{43.5}$ ergs s⁻¹) has precedent in the comparable low-redshift sample analyzed by Corbin (2000). The GOODS combination of deep *Chandra* and *HST* imaging now suggests a persistent merger-AGN disconnect among moderate-luminosity AGNs out to lookback times nearing the peak of AGN activity in the universe. The limited GOODS solid angle provides too few high-luminosity AGNs to test the Bahcall et al. (1997) conclusions over the same redshift range. This may be remedied by the wider area Galaxy Evolution from Morphology and SEDs project *HST* imaging within the extended CDF-S, where Sanchez et al. (2004) have already noted a higher incidence of merger/interaction among 15 optically selected, $z \sim 0.5$ – 1.1 , type 1 AGNs with luminosities spanning the Seyfert/quasar boundary.

Our comparison of the near-neighbor frequency histograms for AGNs and non-AGNs yields a large χ^2 -test probability of the null hypothesis both for the $d < 3r_p$ threshold [$P(\chi^2) = 0.84$] and the $d < 8''$ threshold [$P(\chi^2) = 0.58$]. We note that the $\sim 2\sigma$ discrepancy in near-neighbor frequency previously observed in G03 is no longer apparent for the substantially enlarged samples of the current work. We conclude that local environment, like host asymmetry, is not well correlated with AGN activity. This result, among moderate-redshift AGNs, now extends similar findings of environment-AGN disconnect at low redshift from recent analyses of the Southern Sky Redshift Survey (Maia, Machado, & Willmer 2003) and the SDSS (Miller et al. 2003).

We acknowledge support for this work provided by NASA through GO grants GO-09425 and GO-09583 from the Space Telescope Science Institute, which is operated by AURA, Inc., under NASA contract NAS 5-26555. We thank the anonymous referee for helpful comments.

REFERENCES

- Alexander, D. M., et al. 2003, AJ, 126, 539
Bahcall, J. N., et al. 1997, ApJ, 479, 642
Barger, A. J., et al. 2003, AJ, 126, 632
———. 2005, AJ, 129, 578
Brandt, W. N., et al. 2001, AJ, 122, 2810
Cohen, J. G., et al. 2000, ApJ, 538, 29
Conselice, C. J. 2003, ApJS, 147, 1
Conselice, C. J., et al. 2003, AJ, 126, 1183
Corbin, M. R. 2000, ApJ, 536, L73
Fernandez-Soto, A., Lanzetta, K. M., & Yahil, A. 1999, ApJ, 513, 34
Ferrarese, L. & Merritt, D. 2000, ApJ, 539, 9
Gebhardt, K., et al. 2000, ApJ, 539, 13
Giacconi, R., et al. 2002, ApJ, 139, 369
Giavalisco, M., et al. 2004, ApJ, 600, L93
Graham, A. W., et al. 2001, ApJ, 563, L11
Grogin, N. A., et al. 2003, ApJ, 595, 685 (G03)
Kauffmann, et al. 2003, MNRAS, 346, 1055
Koekemoer, et al. 2002, ApJ, 567, 657
Magorrian, J., et al. 1998, AJ, 115, 2285
Maia, M. A. G., Machado, R. S., & Willmer, C. N. A. 2003, AJ, 126, 1750
Merloni, A., Heinz, S., & Di Matteo, T. 2003, MNRAS, 345, 1057
Miller, C. J., et al. 2003, ApJ, 597, 142
Mobasher, B., et al. 2004, ApJ, 600, L167
Ravindranath, S., et al. 2004, ApJ, 604, L9
Sanchez, S. F., et al. 2004, ApJ, 614, 586
Szokoly, G. P., et al. 2004, ApJS, 155, 271
Walker, I. R., Mihos, J. C., & Hernquist L. 1996, ApJ, 460, 121
Woo, J-H. & Urry, M. C. 2002, ApJ, 579, 530